

Studying Thin Ge Films and Ge/GeO₂ Interfaces by Means of Raman–Brillouin Scattering

L. Yaacoub^a, S. Schamm-Chardon^a, N. N. Ovsyuk^b, A. Zwick^a, and J. Groenen^a

^aCEMES-CNRS and Universite de Toulouse, 31055 Toulouse, France

^bSobolev Institute of Geology and Mineralogy, Novosibirsk, 630090 Russia

e-mail: ovsyuk@igm.nsc.ru

Abstract—The high frequency acoustic phonons employed in Raman–Brillouin scattering are used to probe native oxide layers on Ge film surfaces in GeO₂/Ge/In_xGa_{1-x}As heterostructures. The thermal instability of GeO₂ results in the production of GeO gas on Ge surfaces; molecules of this gas evaporate through the porous GeO₂ layers. As a result, the Ge/GeO₂ interface is depleted of Ge, and a sub-stoichiometric GeO_x layer is formed. By comparing photoelastic modeling and experimental results, we discovered a 0.5 nm thick interfacial region between the film and the oxide, demonstrating the sensitivity of acoustic phonons to the sub-nanometer scale.

DOI: 10.3103/S1062873815110246

INTRODUCTION

Germanium is of growing interest as an alternative to silicon in electronics, due to its high carrier mobility, lower working voltage, and lower processing temperatures. In order to benefit from these properties in devices, we must control the quality of interfacial Ge/GeO₂ layers [1]. Theoretical and experimental studies aimed at gaining a detailed understanding of the electronic and structural properties of Ge/GeO₂ interfaces were described in [2–5]. Infrared Fourier spectroscopy was used to show that upon oxidation in air, sub-stoichiometric GeO_x films are created that then transform into GeO₂ [2]. The local structure around Ge atoms and the electrostatic inhomogeneity in Ge/GeO₂ are usually studied via X-ray photoelectron spectroscopy (XPS) [3]. The atomic structure of Ge/GeO₂ interfaces is then analyzed by comparing the kinks in the valence band via the XPS of chemical shifts and calculating these shifts by means of hybrid functional density [4, 5]. However, the problem of the actual band structure of Ge/GeO₂ interfaces remains open [5].

In this work, we show that Raman–Brillouin (RB) scattering on acoustic phonons can be used to probe super-thin germanium oxide layers in GeO₂/Ge/In_xGa_{1-x}As heterostructures. Since an oxide layer thickness of several nm does not contribute significantly to RB scattering, we study its effect on Raman scattering (RS) generated in a thin Ge film with this layer. Acoustic phonons passing through these layers, including the InGaAs substrate, are sensitive to the medium surrounding the Ge film, allowing us to investigate the influence of this medium on RB scattering in a Ge film. High-frequency acoustic phonons are needed to study the structure on the nanometer scale. Previous

studies of RB scattering on quantum dots and thin films showed that the more localized electronic states participate in RB scattering, while higher-frequency acoustic phonons contribute to the spectra [6–8]. We chose to use the optimum Ge film thickness of 25 nm for RB scattering and then performed numerical simulations of the experimental data.

In this work, we studied the native oxide that formed on the Ge surface. Ge was precipitated on a In_{0.12}Ga_{0.88}As layer that was part of InGaAs/GaAs (001) pseudo-substrate initially intended for engineering under pressure. Introducing tensile biaxial tension in the Ge layer seemed to be an interesting way of increasing carrier mobility and controlling the band gap. The In_{0.12}Ga_{0.88}As layer was grown to a thickness of 1 μm in order to ensure complete elastic relaxation on its surface and the subsequent pseudomorphic growth of strained Ge films. A detailed description of film growth can be found in [9].

Ge layer thickness e was measured via high resolution electron transmission microscopy. Visualization was performed using an FEI Tecnai F20 field emission electron microscope operating at 200 kV and equipped with a spherical aberration corrector designed for direct observation of atomic structures at interfaces with appreciably reduced delocalization contrast of images. It was found from image analysis that $e = 25.5 \pm 0.5$ nm (Fig. 1). An amorphous GeO₂ layer can also be seen in the figure; it is darker than the glue. Due to blurring, however, it is hard to determine the upper boundary of the oxide with subnanometer precision.

Raman–Brillouin scattering was excited at room temperature using line $\lambda = 568.2$ nm of a Kr ion laser. The scattered light was studied using a Horiba Jobin

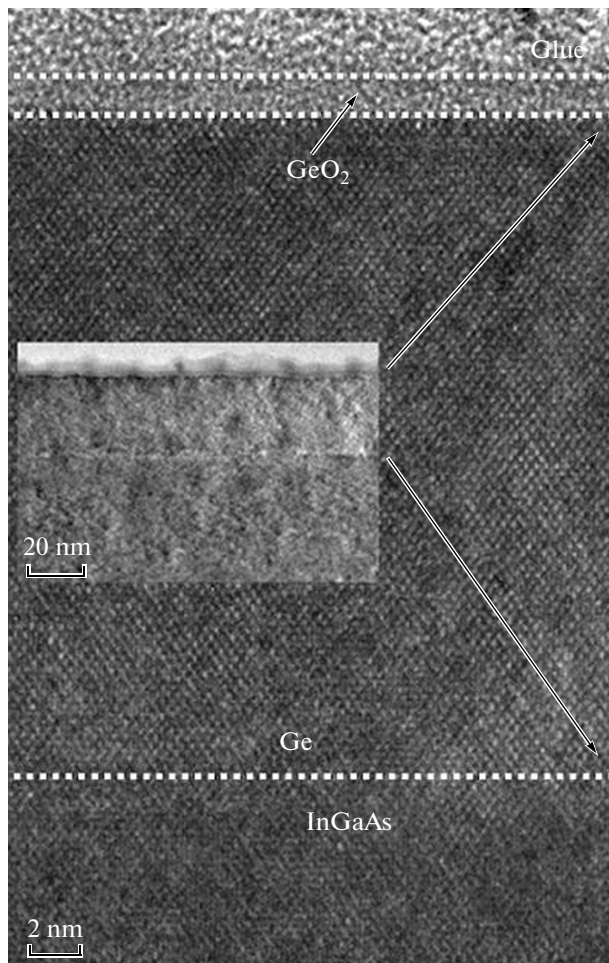


Fig. 1. Heterosystem $\text{GeO}_2/\text{Ge}/\text{InGaAs}$ $\langle 110 \rangle$ obtained via high-resolution transmission electron microscopy. The layer of glue used in sample preparation can be seen on the oxide surface.

Yvon T64000 micro-Raman spectrometer equipped with a CCD camera. In contrast to conventional RS micromessurements, the incident exciting laser beam and collected scattered light had no common path; the laser was focused by an objective mounted off-axis with respect to the collecting objective. This meant the reflected beam was not incident on the spectrometer and did not cause Rayleigh scattering. Instead, we deal with an internal quasi-backscattering configuration, due to the high Ge refractive index ($n = 5.34$).

The calculated RB spectra presented in this work were simulated using a general formulation of the photoelastic model described in [7]. This model included the spatial modulation of elastic, photoelastic, and optical properties. The scattering of the longitudinal acoustic mode polarized along growth axis z was calculated. All calculated spectra were convolved using a Gaussian (FWHM 0.8 cm^{-1}) in order to allow for experimental resolution. The numerical values of the densities, speeds of sound, and refractive indices used

in the simulation were taken from [10] for Ge, GaAs, and InGaAs, and from [11] for GeO_2 .

We knew from our previous studies with Si monolayers that RB scattering is a result of the combined action of acoustic, optical, and photoelastic cavities [7, 8]. It is interesting that acoustically, Ge and $\text{In}_{0.12}\text{Ga}_{0.88}\text{As}$ are virtually identical to one another; their acoustic impedances (the product of their density and the speed of sound) differ by just 1%. The absence of acoustic cavity due to the interface between Ge and $\text{In}_{0.12}\text{Ga}_{0.88}\text{As}$ therefore greatly simplifies the analysis of experimental data. The optical parameters of Ge and $\text{In}_{0.12}\text{Ga}_{0.88}\text{As}$ are also quite close, weakening the contribution from the optical cavity effect in RB scattering. At wavelength $\lambda_i = 568.2 \text{ nm}$, a Ge film is selectively excited in resonance with the E_1 transition in Ge, ensuring a strong photoelastic response. In contrast, the photoelastic response in ultrathin transparent GeO_2 layer is negligible. Unlike Ge, this wavelength of exciting light is not a resonance wavelength for an InGaAs substrate, and the contribution to RB scattering from InGaAs is thus relatively weak. In addition, the contribution to RB scattering from the InGaAs is a volume Brillouin peak localized below 5 cm^{-1} , in accordance with the considerable thickness of $1 \mu\text{m}$. This spectral range was not considered in our experiment. We thus considered mainly RB scattering in a Ge film. We therefore assumed in our calculations that the photoelastic effect occurs in Ge films only. This implies that the photoelastic profile $p(z)$ would be constant in a Ge film and zero beyond the film [7].

Let us first consider a simple example in which the Ge/InGaAs/GaAs heterostructure is not covered with oxide. The corresponding RB scattering spectrum is shown in the lower part of Fig. 2. A strong peak below 10 cm^{-1} and a number of regularly spaced peaks whose intensities rapidly decline as the energy grows are observed in this spectrum. In accordance with the above, these peaks are not associated with acoustic resonances in the Ge film because the Ge/ $\text{In}_{0.12}\text{Ga}_{0.88}\text{As}$ interface does not form an acoustic resonator. Since the optical cavity effects are also weak, we considered a simplified version of the photoelastic model (Eq. (2) in [7]). For a simple standing acoustic wave resulting from total reflection off a sample surface, the scattering efficiency as a function of wave vector \vec{q} is proportional to the expression

$$I(q) \propto \left\{ \text{sinc}^2 \left[(\Delta k - q) \frac{e}{2} \right] + \text{sinc}^2 \left[(\Delta k + q) \frac{e}{2} \right] - 2 \cos(qe) \text{sinc} \left[(\Delta k - q) \frac{e}{2} \right] \text{sinc} \left[(\Delta k + q) \frac{e}{2} \right] \right\}, \quad (1)$$

where Δk is the variation in the photon wave vector. Cardinal sine $\text{sinc}(Q) = \sin(Q)/Q$ is associated with the Fourier transform of rectangular photoelastic profile

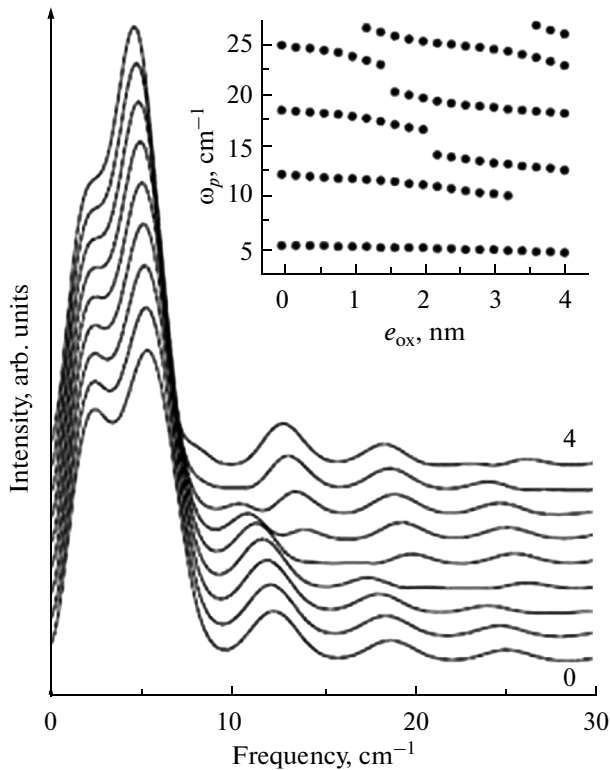


Fig. 2. RB spectra calculated for our 25.5 nm thick Ge film covered with an oxide layer whose thickness e_{ox} varied from (lower) 0 to (upper) 4 nm with steps of 0.5 nm. The insert shows the peak maxima ω_p as functions of thickness e_{ox} .

$p(z)$ [7]. The Stokes RB spectrum dominates in the first term of Eq. (1) (associated with the cardinal sine, it is concentrated at $q = \Delta k$). This results in rapidly decaying peaks with pseudo-periodicity $2\pi/e$ of the wave vector [7]. Equation (1) and the complete calculation (lower spectrum in Fig. 2) do yield the same peak positions.

Below, we assume that Ge film behaves as a source of RB scattering, allowing us to study the parameters of the oxide layer on its surface; the layer does not produce its own RB scattering. To describe the role played by cavities in the new configuration, we need the photoelastic model in the general formulation in [7]. Figure 2 shows a number of spectra calculated with GeO₂ thickness e_{ox} in the interval of 0.5 to 4 nm with steps of 0.5 nm. Adding the oxide to the Ge film's surface changes the RB spectra appreciably. As e_{ox} gradually increases, some peaks fade out while others appear. The insert in Fig. 2 shows that as e_{ox} grows, the peak positions shift downward with respect to energy. Figure 2 demonstrates that RB scattering is highly sensitive to the presence of oxide and its thickness. The dependence on e_{ox} is mainly determined by acoustic and photoelastic effects. As an oxide layer appears on the surface, the boundary conditions for the acoustic displacement fields are changed, and the

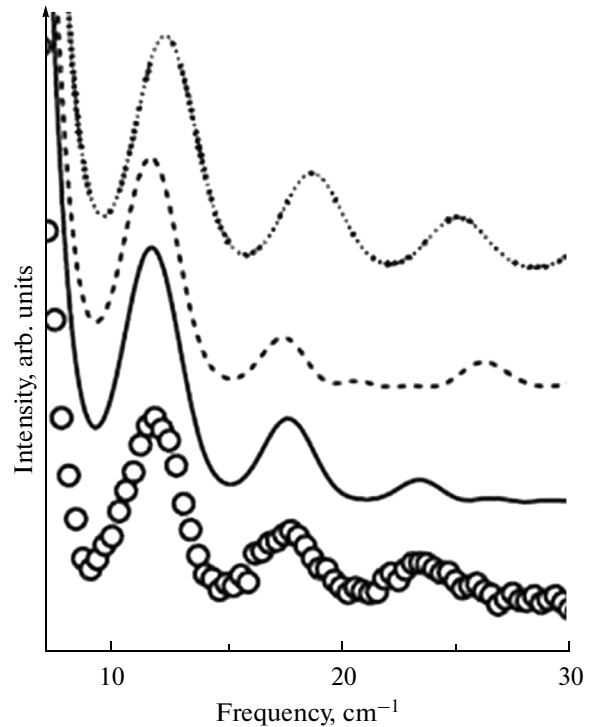


Fig. 3. (Dots) experimental RB spectrum and calculated spectra for our 25.5 nm thick Ge film: (dotted line) without oxide, (dashed line) with 1.5 nm thick oxide; and (solid line) with a 0.5 nm thick interface region and a 1.0 nm thick oxide layer.

free surface corresponds to the upper oxide surface. As e_{ox} increases, the acoustic displacement fields gradually change phase with respect to the Ge film, and thus to photoelastic profile $p(z)$. The conditions responsible for the RB scattering maxima therefore change as well, and peaks are observed at other wavenumbers. Similar effects that an oxide layer has on RB scattering were observed for layers of ultrathin superlattices and quantum dots in [12, 13].

Our experimental spectrum is shown in Fig. 3. Three pronounced peaks can be observed within the interval of 10–30 cm⁻¹. The calculated spectrum indicated by the dotted line corresponds to a 25.5 nm thick Ge film with no oxide on its surface. The three calculated peaks correspond to higher frequencies than the experimental ones. Figure 2 shows that adding a thin oxide surface layer changes the RB spectra appreciably. At different thicknesses of e_{ox} , the best agreement with experiment was obtained when $e_{\text{ox}} = 1.5$ nm (dashed line in Fig. 3), for which the first two peaks were the same as the experimental ones. Above 20 cm⁻¹, the calculations are however unsatisfactory, as they yielded an almost flat line in place of the third experimental peak.

Acoustic waves with short wavelengths λ_{ac} are very sensitive to small variations. For 23 cm⁻¹ (i.e., at the

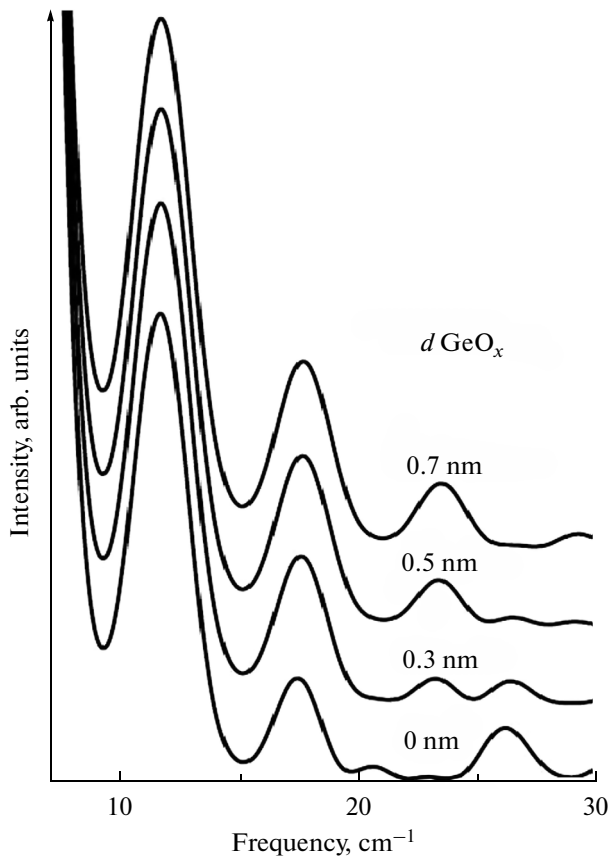


Fig. 4. RB spectra for different interface region thicknesses. From the bottom up: a 1.5 nm thick GeO_2 layer with no interface region; a 1.2 nm thick oxide layer with a 0.3 nm thick interface region; a 1.0 nm thick oxide layer with a 0.5 nm thick interface region; and a 0.8 nm thick oxide layer with a 0.7 nm thick interface region.

maximum of the third experimental peak), the acoustic phonons in Ge had acoustic wavelength $\lambda_{ac} = 7$ nm. Since λ_{ac} corresponds to a phase variation of 2π , the 0.5 nm change in the oxide thickness resulted in a notable 0.143π change of phase, i.e., by 0.45 radian. This demonstrates that such high frequency acoustic waves can detect nanometer and even sub-nanometer variations.

This compelled us to investigate further details beyond the structural analysis allowed by high resolution electron microscopy. It is known that in order to calculate the band shift at a Ge/ GeO_2 interface, we must introduce a sub-stoichiometric interfacial layer [4]. This layer emerges because GeO gas is formed at Ge/ GeO_2 interface, and molecules of this gas evaporate through the porous GeO_2 . As a result, this interface is depleted of germanium, and a sub-stoichiometric GeO_x region appears. We calculated the RB spectra for a 25.5 nm thick Ge film covered with an oxide layer with thickness e_{ox} and an interface region thickness varying such that the total thickness was equal to 1.5 nm (Fig. 4). We found that good agreement

between simulations and experiments can be achieved by introducing an ultrathin interfacial layer (IL) with a thickness of 0.5 nm between the GeO_2 and Ge film. This spectrum is indicated by the solid line in Fig. 3. For simplicity, we assume that it has average properties between those of Ge and GeO_2 ; i.e., density $\rho(\text{IL}) = 0.5[\rho(\text{Ge}) + \rho(\text{GeO}_2)]$. With this layer, the positions of the first two peaks remained virtually unchanged, while the changes at higher frequencies were considerable. In particular, an almost flat line was transformed into a third peak that agreed with the experimental peak at 23 cm^{-1} .

In accordance with our RB scattering simulation, an experimental spectrum was obtained from the following structure: an InGaAs substrate was covered with a 25.5 nm thick Ge film, a 0.5 nm thick interfacial layer, and finally a 1 nm thick GeO_2 layer. The total thickness of the interfacial and oxide layers was 1.5 nm. This agreed with the amorphous layer shown in Fig. 1. Note that the band shift at Ge/ GeO_2 interface was calculated with a hybrid density functional using a 0.6 nm thick sub-oxide layer [4]. The thickness of this transition layer agreed with that of our interfacial layer, as was confirmed experimentally.

CONCLUSIONS

RB scattering generated in a thin Ge film was studied in order to probe a GeO_2 layer and a Ge/ GeO_2 interface. Since acoustic phonons that participate in scattering are sensitive to the Ge layer environment, we could not only determine the native oxide's thickness but the presence of an interfacial layer at the Ge/ GeO_2 boundary as well. This is important both in characterizing the GeO_2 layer and Ge/ GeO_2 interface, and as additional information on the local structure obtained via XPS. Sensitivity on the sub-nanometer scale was demonstrated. High frequency acoustic phonons are especially sensitive to the actual nature of the interface. In the end, the variation in acoustic impedance upon crossing the interface determines the degree of reflection of acoustic waves. We showed that materials with low RB scattering intensity can nonetheless be investigated under the condition that nanometer thick films in which RB scattering is produced are used as an internal probe.

REFERENCES

1. Houssa, M., Satta, A., Simoen, E., Jaeger, B.D., Meuris, M., Caymax, M., and Heyns, M., in *Germanium-Based Technologies*, Oxford: Elsevier, 2007.
2. Park, K., Lee, Y., Lee, J., and Lim, S., *Appl. Surf. Sci.*, 2008, vol. 254, p. 4828.
3. Prabhakaran, K. and Ogino, T., *Surf. Sci.*, 1995, vol. 325, p. 263.
4. Broqvist, P., Binder, J.F., and Pasquarello, A., *Appl. Phys. Lett.*, 2009, vol. 94, p. 141911; Broqvist, P.,

- Binder, J.F., and Pasquarello, A., *Appl. Phys. Lett.*, 2011, vol. 98, p. 129901.
5. Binder, J.F., Broqvist, P., Komsa, H.P., and Pasquarello, A., *Phys. Rev. B*, 2012, vol. 85, p. 245305.
 6. Mlayah, A. and Groenen, J., in *Light Scattering in Solids IX*, Cardona, M. and Merlin, R., Eds., Berlin, Heidelberg: Springer-Verlag, 2007.
 7. Groenen, J., Poinsothe, F., Zwick, A., Sotomayor-Torres, C.M., Prunnila, M., and Ahopelto, J., *Phys. Rev. B*, 2008, vol. 77, p. 045420.
 8. Lou, N., Groenen, J., Benassayag, G., and Zwick, A., *Appl. Phys. Lett.*, 2010, vol. 97, p. 141908.
 9. Bolkhovityanov, Yu.B., Vasilenko, A.P., Gutakovskii, A.K., Deryabin, A.S., Putyato, M.A., and Sokolov, L.V., *Phys. Solid State*, 2011, vol. 53, p. 2005.
 10. Levinshtein, M., Rumyantsev, S., and Shur, M., *Handbook Series on Semiconductor Parameters*, Singapore: World Sci., 1996, vol. 1.
 11. Antoniou, A. and Morisson, J.A., *J. Appl. Phys.*, 1965, vol. 36, p. 1873.
 12. Lockwood, D.J., Dharma-Wardana, M.W.C., Aers, G.C., and Baribeau, J.-M., *Appl. Phys. Lett.*, 1988, vol. 52, p. 2040.
 13. Cazayous M., Groenen J., Huntzinger J.R., Bachelier G., Zwick A., Mlayah A., Bedel-Pereira, E., Negri, F., Carriere, H., Bertru, N., Paranthoen, C., and Dehaese, O., *Phys. Rev. B*, 2004, vol. 69, p. 125323.

Translated by E. G. Baldina